ARTICLES

Dynamics of nucleosome remodelling by individual ACF complexes

Timothy R. Blosser[1,2], Janet G. Yang[3], Michael D. Stone[1,4], Geeta J. Narlikar[3] & Xiaowei Zhuang[1,4,5]

The ATP-dependent chromatin assembly and remodelling factor (ACF) functions to generate regularly spaced nucleosomes, which are required for heritable gene silencing. The mechanism by which ACF mobilizes nucleosomes remains poorly understood. Here we report a single-molecule FRET study that monitors the remodelling of individual nucleosomes by ACF in real time, revealing previously unknown remodelling intermediates and dynamics. In the presence of ACF and ATP, the nucleosomes exhibit gradual translocation along DNA interrupted by well-defined kinetic pauses that occurred after approximately seven or three to four base pairs of translocation. The binding of ACF, translocation of DNA and exiting of translocation pauses are all ATP-dependent, revealing three distinct functional roles of ATP during remodelling. At equilibrium, a continuously bound ACF complex can move the nucleosome back-and-forth many times before dissociation, indicating that ACF is a highly processive and bidirectional nucleosome translocase.

The packaging of DNA into chromatin represses essential nucleic acid transactions, such as transcription, replication, repair and recombination. This repression is in part regulated by chromatin remodelling enzymes, which couple the energy of ATP hydrolysis to the assembly and mobilization of nucleosomes. ATP-dependent chromatin remodelling enzymes can be classified into several subfamilies, SWI/SNF, ISWI, CHD/Mi2 and INO80, depending on their composition and function[1–5]. Despite possessing a conserved superfamily 2 ATPase subunit that facilitates DNA translocation[6,7], different subfamilies exhibit divergent remodelling activities. For example, the ISWI enzymes have been shown to translocate the histone octamer along DNA and generate a repositioned nucleosome with a canonical structure[8–11], whereas the SWI/SNF enzymes generate a variety of products including repositioned nucleosomes, alternative nucleosome structures containing DNA loops, and nucleosomes with altered histone composition[1–5]. The kinetic intermediates and pathways through which the nucleosome structure evolves during remodelling, however, remain largely elusive. Single molecule experiments are ideally suited to probe these dynamics. Recently, optical and magnetic tweezers have been used to study individual SWI/SNF remodellers, providing direct measurements of DNA translocation and loop formation by these enzymes[12–14]. In this work, we established a single-molecule fluorescence resonance energy transfer (FRET)[15–17] assay to characterize the structural dynamics and kinetic intermediates of nucleosomes during remodelling. Human ACF[18–22], a representative member of the ISWI family of remodellers, was investigated using this approach.

Probing nucleosome translocation by FRET

For FRET characterizations, we labelled histone octamers with a donor dye (Cy3) on histone H2A (ref. 23) and reconstituted mononucleosomes with the Cy3-labelled octamer and a double-stranded DNA that contained an acceptor dye (Cy5) and a biotin at opposite ends. Unless otherwise indicated, we used the 601 nucleosome positioning sequence[24] to place the octamer three base pairs (bp) away from the Cy5-labelled exit end of the DNA, leaving 78 bp of linker DNA on the entry side (Fig. 1a, Supplementary Fig. 1a, $n = 3$ bp). The nucleosomes were then anchored to a microscope slide via a biotin–streptavidin linkage and imaged by a total-internal-reflection-fluorescence (TIRF) microscope[25]. The presence of two H2A subunits in each octamer led to a heterogeneous population of nucleosomes with three different labelling configurations: (1) donor on the H2A subunit proximal to the acceptor, (2) donor on the H2A subunit distal to the acceptor, (3) donor on both H2A subunits. Single-molecule detection allowed these configurations to be discriminated. Three distinct peaks centred at FRET = 0.88, 0.75 and 0.58 were observed in the FRET distribution (Fig. 1b). The assignment of these peaks to the three labelling configurations was further confirmed by individual FRET time traces, which showed one- or two-step photobleaching for nucleosomes bearing one or two donor dyes, respectively (Supplementary Fig. 2). In the following, we focus our analyses on nucleosomes containing a single donor on the proximal H2A (FRET = 0.88) to maximize the dynamic range in our experiments.

Recombinant ACF, comprised of a catalytic ATPase subunit, SNF2h, and an accessory subunit, Acf1(also known as SMARCA5 and BAZ1A, respectively) [19–22], was added to the surface-anchored nucleosomes to induce remodelling. FRET decreased substantially on addition of ACF and ATP (Fig. 1b), whereas incubation with ACF alone resulted in no significant change in FRET (data not shown). The observed decrease in FRET is consistent with the ability of ACF to centre mononucleosomes on DNA[10,11,23,26,27] (Fig. 1a). The average remodelling rate measured from nucleosomes anchored to the surface was quantitatively similar to that determined from measurements of nucleosomes in solution, indicating that surface-anchoring of nucleosomes did not inhibit the activity of ACF (Supplementary Fig. 3).

In order to correlate the observed FRET value to the octamer position quantitatively, we measured FRET for a series of nucleosome constructs with different linker DNA lengths (n) on the exit side (Fig. 1c). The FRET value decreased monotonically with increasing exit linker length in a manner similar to the distance-dependence of FRET observed between donor and acceptor dyes attached to a DNA duplex (Supplementary Fig. 4). To test further whether the ACF-induced

[1]Howard Hughes Medical Institute, [2]Graduate Program in Biophysics, Harvard University, Cambridge, Massachusetts 02138, USA. [3]Department of Biochemistry and Biophysics, University of California, San Francisco, California 94107, USA. [4]Department of Chemistry and Chemical Biology, [5]Department of Physics, Harvard University, Cambridge, Massachusetts 02138, USA.

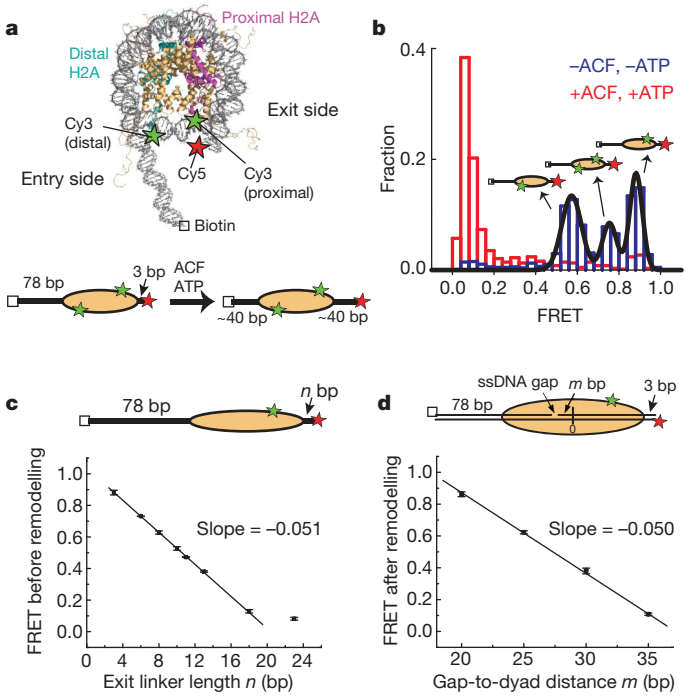

Figure 1 | Monitoring ACF-catalysed nucleosome remodelling by single-molecule FRET. a, The nucleosome structure[33] is shown (upper panel) with labelling sites for Cy3 and Cy5 indicated by green and red stars, respectively. Additional B-form DNA is modelled onto the entry and exit sides of the nucleosome to show the flanking DNA linkers. A linear nucleosome scheme (lower panel) showing the footprint of the histone octamer (yellow oval) on the DNA (black line) before and after ACF-catalysed remodelling. **b**, The FRET distribution of the $n = 3$ bp nucleosomes before (blue bars) and after (red bars) remodelling. The three initial peaks centred at FRET = 0.88, 0.75 and 0.58 (derived from Gaussian fit, black line) result from the three distinct Cy3-labelling configurations. After equilibration with ACF and ATP, the FRET values reduce to below 0.1. **c**, The initial FRET value as a function of the exit linker DNA length (n). The data were fit to a line with a slope of -0.051 ± 0.002 (black line). The last point near zero FRET is excluded from the linear fit. In this and subsequent figures, data from nucleosomes with a single Cy3 dye on the proximal H2A subunit are presented. The selection criteria for these nucleosomes are described in Methods. **d**, The final FRET values after remodelling by ACF as a function of m, the number of base pairs between the ssDNA gap and the nucleosome dyad (denoted as 0). The linear fit (black line) gives a slope of -0.050 ± 0.002. Error bars are ± s.e.m.

FRET change was indeed due to translocation of the histone octamer on DNA, we designed nucleosomes with stall sites defined by single-stranded (ss) DNA gaps. It has been shown that the ATPase domain of ISWI remodellers contacts a DNA region two helical turns (~20 bp) from the dyad axis of the nucleosome, and that ssDNA gaps located in this region inhibit nucleosome translocation[28–30]. We thus prepared a series of nucleosomes with the same linker DNA lengths (78 bp on the entry side and 3 bp on the exit side), each possessing a two-nucleotide ssDNA gap at a specified distance (m bp) away from the dyad axis (Fig. 1d). Although the initial FRET values of these constructs were similar to that observed for the construct without the ssDNA gap, the final FRET values after remodelling showed a strong dependence on the position of the ssDNA gap (Fig. 1d), with little FRET change for the construct with $m = 20$ bp and a final FRET versus m slope identical to that observed for the exit linker length dependence shown in Fig. 1c. These results demonstrate that the observed ACF-induced FRET changes can be quantitatively interpreted in terms of nucleosome translocation along DNA, although we cannot formally exclude the possibility that other alterations in nucleosome structure could also make a minor contribution. An interesting consideration is the spontaneous site exposure owing to fraying DNA ends previously reported to occur in the 0.01–0.05 s time scale[31], which should not cause significant fluctuations in FRET observed here with 0.1–2 s time resolution.

Multiple ATP-dependent remodelling steps

Next we characterized the remodelling kinetics by adding ACF and ATP to the nucleosomes *in situ* during data acquisition. After the addition of ACF and ATP, individual nucleosomes exhibited a 'waiting' period before any detectable change in FRET, followed by a 'translocation' period, during which FRET decreased to the background level (Fig. 2a). The duration of the waiting period (t_{wait}) depended on both ACF and ATP concentrations (Fig. 2b). The distributions of t_{wait} obtained at various ACF and ATP conditions indicate that the waiting phase included at least two steps, one depending on the ACF concentration and the other on ATP (Supplementary Fig. 5). To determine the order of these two steps, we performed a three-colour experiment with dye-labelled ACF, in which signal from the Alexa 488 dye on ACF directly reported the binding of the enzyme, whereas the FRET pair on the nucleosome reported the nucleosome position on the DNA. Notably, the binding of ACF preceded the onset of FRET decrease (Fig. 2c). Both the time before ACF binding (t_{bind}) and the time lag (t_{lag}) from ACF binding to the onset of FRET decrease depended on the ATP concentration (Fig. 2c), indicating that the waiting phase consisted of an ATP-dependent ACF binding step followed by an additional ATP-dependent step after the enzyme bound.

In contrast to the waiting phase, the duration of the translocation phase ($t_{translocate}$) was only dependent on ATP but not on ACF concentration (Fig. 2d and Supplementary Fig. 6), indicating that binding of additional ACF molecules was not required during this phase. Consistent with this notion, when we prebound nucleosomes with ACF and then removed unbound ACF with a buffer containing ATP but not ACF to initiate remodelling, the majority (86%) of the remodelled nucleosomes showed a complete decrease in FRET to below 0.1, indicating that the translocation phase did not require binding of additional ACF from the solution.

Translocation pauses during remodelling

Notably, translocation of the nucleosome did not proceed at a constant rate. Instead, the translocation phase exhibited periods of gradual decrease in FRET interrupted by translocation pauses (Fig. 3). For nucleosomes with the initial exit linker length $n = 3$ bp, the first pause occurred at a FRET value of 0.53 ± 0.03 (Fig. 3a, b), corresponding to an increase of linker length to 9.9 ± 0.6 bp and thus nucleosome translocation by 6.9 ± 0.6 bp. The pause position seemed to be independent of the initial linker length: for nucleosome constructs with four different linker DNA lengths ($n = -3$, 0, 3 and 6 bp), the first pause all occurred after approximately 7 bp of DNA translocation (Supplementary Fig. 7a).

In addition, we tested the dependence of the pause position on DNA sequence using a weaker positioning sequence 'A-100' (Supplementary Fig. 1b), which has ~100 fold lower affinity than the 601 sequence[32]. The first pause of these nucleosomes again occurred after approximately 7 bp of translocation (Supplementary Fig. 7b). Although we cannot formally rule out the possibility that the positioning sequences contributed to the position of this initial pause, the observation that nucleosomes with two substantially different DNA sequences exhibit the same initial pause position indicates a potentially general feature of remodelling by ACF.

In addition to the first pause, subsequent translocation pauses were observed at lower FRET values (Fig. 3a, c). For nucleosomes with initial exit linker length $n = 3$ bp, a second and third pause preferentially occurred at FRET = 0.34 ± 0.03 and 0.17 ± 0.03, corresponding to 3.8 ± 0.6 bp and 3.3 ± 0.6 bp of translocation before pausing, respectively (Fig. 3a, b). Similar pauses were also observed for the $n = -3$ bp nucleosomes, except that the shorter exit linker length after the third pause allowed detection of a fourth pause, which occurred after 3.6 ± 0.8 bp of translocation from the third pause (Figs 3c, d). Taken together, these results indicate that the nucleosomes were translocated by a shorter distance (3–4 bp) between the subsequent pauses. Both the dwell time of the pauses and the duration of the translocation phases in between pauses

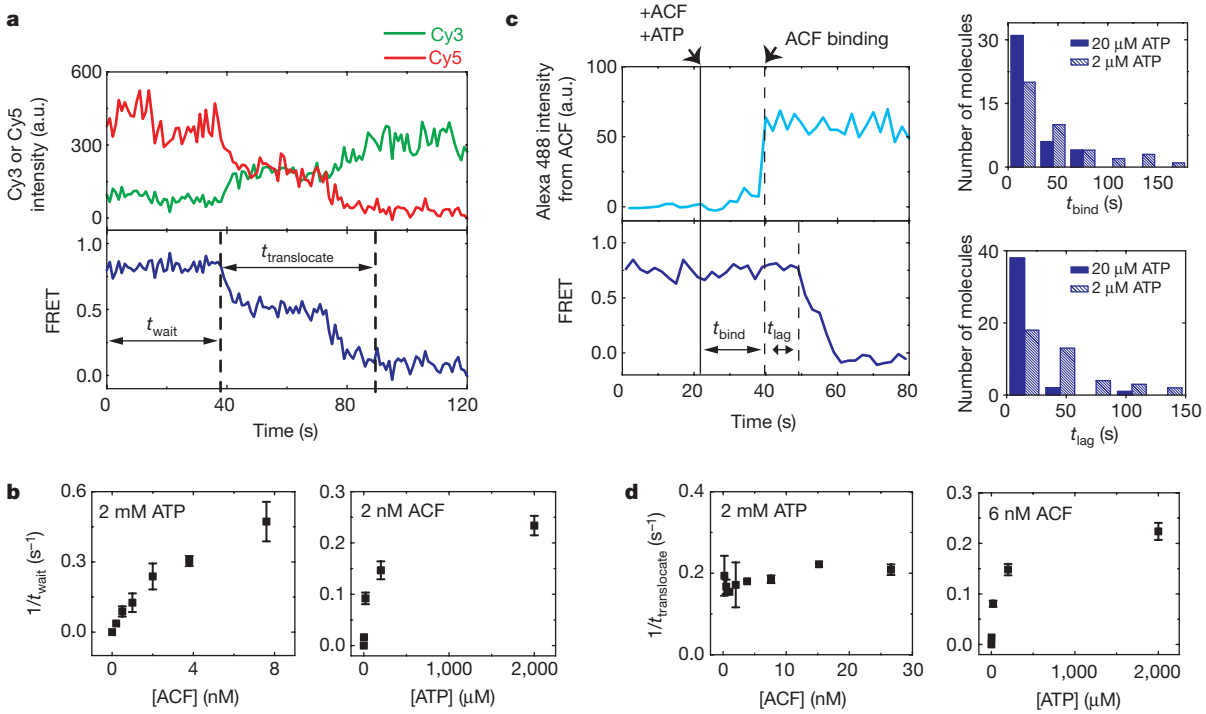

Figure 2 | Real-time dynamics of ACF-catalysed nucleosome translocation. **a**, Donor fluorescence (green), acceptor fluorescence (red) and FRET (blue) traces showing the ACF-induced remodelling of a single nucleosome ($n = 3$ bp). ACF (6 nM) and ATP (2 μM) were added at time zero. The durations of the waiting phase and the translocation phase are denoted as t_{wait} and $t_{translocate}$, respectively. a.u., Arbitrary units. **b**, Dependence of the mean t_{wait} value on ACF and ATP concentrations. **c**, Simultaneous monitoring of the binding of ACF and the remodelling of nucleosomes. Left panels: the upper trace shows the fluorescence signal from the Alexa 488-labelled ACF; the lower trace shows FRET between Cy3 and Cy5 on the nucleosome. ACF (4 nM) and ATP (20 μM) were added at the time indicated by the solid black line. The binding event of ACF (indicated by the first dashed line) further divides t_{wait} into two phases, t_{bind} and t_{lag}. Right panels: the distributions of t_{bind} and t_{lag} at two different ATP concentrations and 4 nM ACF. The distributions at different ATP concentrations are statistically distinct with 95% confidence for t_{bind} and more than 99% confidence for t_{lag} according to the Kolmogorov–Smirnov test. **d**, Dependence of the mean $t_{translocate}$ value on ACF and ATP concentrations. Error bars are ± s.e.m.

depended on the concentration of ATP, indicating that ATP binding was required in both phases (Fig. 3e and Supplementary Fig. 8). The dwell times of the subsequent pauses were similar to each other but substantially shorter than that of the first pause.

We note that the sum of a 7 bp and a 3–4 bp step and the sum of three 3–4 bp steps are both close to the 10 bp periodicity of DNA–histone contacts within the nucleosome[33]. Interestingly, the remodelling intermediates at a fraction of the periodicity (7 bp and 3–4 bp) were not stable in the absence of the remodelling enzyme: after removal of ACF, these intermediates collapsed to nucleosomal states in which the histone octamer was repositioned by a multiple of ~10 bp from the pre-remodelling position (Supplementary Fig. 9). These collapsed states, consistent with the previously observed accumulation of remodelling products at ~10 bp intervals of nucleosome translocation[28,29], are probably imposed by structural constraints of the nucleosome.

Processive and bidirectional translocation

The above experiments with end-positioned nucleosomes provide quantitative analyses of remodelling kinetics and intermediates. The limited dynamic range of FRET, however, made it difficult to characterize the equilibrium state(s) after remodelling using these substrates. Considering that ACF tends to centre the nucleosome on the DNA, we reasoned that a centre-positioned nucleosome with an initial FRET value within the dynamic range of FRET would facilitate the analysis of equilibrium remodelling dynamics. To this end we constructed a centre-positioned mononucleosome with the 601 sequence flanked by 78 bp of DNA on each side and an internal acceptor label (Fig. 4a, Supplementary Fig. 1a). The initial FRET distribution showed a narrow peak at FRET = 0.3 (Supplementary Fig. 10). After equilibration with ACF and ATP, the FRET distribution broadened substantially (Supplementary Fig. 10) and the time traces of individual nucleosomes exhibited large-amplitude oscillations in FRET (Fig. 4b), indicating that the histone octamer was translocated back-and-forth along the DNA by the remodelling enzyme. Bidirectional remodelling was observed to be the predominant behaviour (>70% of remodelled nucleosomes), even at sub-saturating conditions in which a low concentration (1 nM) of ACF was added to induce remodelling of only a small fraction (<10%) of the nucleosomes. Autocorrelation analysis of these FRET time traces showed a characteristic oscillation time that was dependent on the ATP concentration but independent of the ACF concentration (Fig. 4b), indicating that the observed bidirectional translocation was accomplished by continuously bound ACF without requiring dissociation and rebinding of ACF from the solution. To test further this notion, we performed three-colour experiments with Alexa 488-labelled ACF and FRET-labelled nucleosomes, in which signal from the Alexa 488 dye directly reported the binding of ACF. Repeated back-and-forth movement of the nucleosomes was observed within individual ACF binding events (Supplementary Fig. 11), further confirming that the bidirectional nucleosome translocation was accomplished by a continuously bound ACF complex.

To quantify further the processivity of ACF, we performed buffer exchange experiments in which ACF and ATP were added and unbound ACF (but not ATP) was subsequently removed *in situ* as the position of individual nucleosomes was monitored. Notably, the ACF-induced bidirectional movement persisted for a long period of time after unbound ACF was removed from the solution (Fig. 4c). The nucleosomes were translocated with an average speed of approximately 2 bp s^{-1}. The lower-bound estimate of the cumulative distance travelled by the nucleosome after removal of unbound ACF exhibits a broad distribution with a mean of 200 bp (Fig. 4c). Taken together, these results indicate that ACF is a highly processive and bidirectional nucleosome translocase. The observed processivity is consistent with the strong commitment of ISWI enzymes to nucleosomal templates once chromatin assembly and remodelling are initiated[34,35].

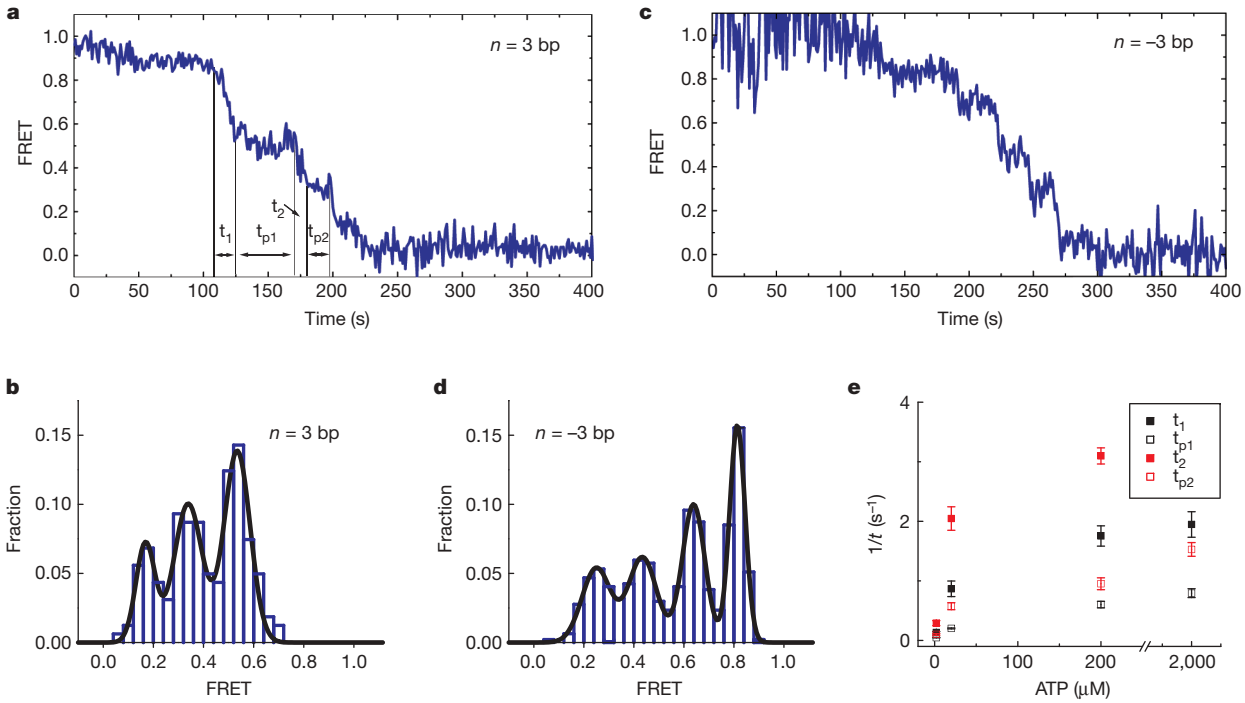

Figure 3 | ACF-catalysed nucleosome translocation is interrupted by well defined kinetic pauses. **a**, FRET time trace of a nucleosome ($n = 3$ bp) showing kinetic pauses that divide the entire translocation phase into several translocation and pause sub-phases: t_1, t_{p1}, t_2, t_{p2}… ACF (6 nM) and ATP (2 μM) were added at time zero. **b**, FRET distribution of the pauses constructed from many $n = 3$ bp nucleosomes. The peak FRET values, 0.53, 0.34, and 0.17 (obtained from Gaussian fit, black line), correspond to 6.9 bp of translocation between the initial position and the first pause, 3.8 bp between the first and second pauses, and 3.3 bp between the second and third pauses. **c**, FRET time trace of a $n = -3$ bp nucleosome after addition of ACF (6 nM) and ATP (2 μM) at time zero. The proximity of the initial donor and acceptor positions causes partial quenching of their fluorescence and thus relatively large fluctuations in initial FRET. **d**, FRET distribution of the pauses constructed from many $n = -3$ bp nucleosomes. The peaks correspond to 7.3 bp of translocation between the initial position and the first pause, 3.4 bp between the first and second pauses, 4.0 bp between the second and third pauses, and 3.6 bp between the third and fourth pauses. **e**, ATP-dependence of the mean t_1, t_{p1}, t_2, and t_{p2} values. Error bars are ± s.e.m.

It is striking that an ACF complex remaining bound to the nucleosome could cause such a highly processive, back-and-forth nucleosome movement. Such a demanding task could be accomplished if ACF preferentially binds the nucleosome as a dimer, in which two ACF monomers, particularly their corresponding ATPase domains, are bound on opposite sides of the nucleosome and oriented for translocation in opposing directions. Coordinated action of the two monomers would then allow processive back-and-forth translocation of the nucleosome. This hypothesis is supported by our three-colour experiments with Alexa 488-labelled ACF and FRET-labelled nucleosomes. To determine the number of ACF bound to the nucleosome, we performed statistical analyses of the Alexa 488 intensity and the number of Alexa 488 photobleaching steps associated with each ACF binding event. These analyses are statistically consistent with the notion that the binding events leading to bidirectional nucleosome remodelling contained two ACF monomers, whereas the binding events leading to unidirectional remodelling contained a single ACF monomer (Supplementary Fig. 12). Further supporting this model, electron microscopy and biochemical data showed cooperative binding of two SNF2h proteins to a single nucleosome with each SNF2h occupying one side of the nucleosome in an activated ATP state[36]. The diffusion coefficient of ACF bound to DNA is also consistent with a complex of two Acf1 and two SNF2h subunits[37]. Interestingly, the SWI/SNF subfamily enzymes can also reversibly create and retract DNA loops[12,13], but it is unclear whether the bidirectional nucleosome translocation by ACF and the reversible DNA loop formation by SWI/SNF share a common mechanism.

Discussion

We have developed a single-molecule assay to monitor the remodelling of individual nucleosomes by chromatin remodelling enzymes in real time. This assay allowed quantitative characterization of the structural dynamics and kinetic intermediates of nucleosomes during remodelling. Using this approach, we showed that the human ACF enzyme induced gradual translocation of nucleosomes along DNA interrupted by well-defined kinetic pauses. ATP has multiple functional roles in the remodelling process. The three distinct steps during remodelling, namely binding of ACF, translocation of the nucleosome and translocation pauses, were all ATP-dependent, demonstrating a versatile usage of ATP by an enzyme with only one type of ATP binding site.

Quantification of the FRET traces of end-positioned nucleosomes showed that the first kinetic pause occurred after approximately 7 bp of nucleosome translocation, whereas subsequent pauses were separated by only 3–4 bp. Although it is currently unclear whether these remodelling intermediates occur only at the beginning of remodelling or continue into the processive remodelling phase, similar translocation pauses were also observed during the continuous remodelling process of centre-positioned nucleosomes (Fig. 4b) and thus may represent a fundamental property of ACF-induced remodelling. One possible origin of these intermediates is an ATP-dependent conformational change of the remodelling enzyme that prepares the nucleosome for the next round of DNA translocation (for example, by forming a DNA loop for subsequent propagation around the nucleosome)[30,38,39]. The unique properties of the first pause, compared to the subsequent pauses, may indicate a complex initiation phase of remodelling.

On centre-positioned nucleosomes, ACF was observed to exhibit remarkable processivity and bidirectionality: an ACF complex continuously bound to a nucleosome could translocate the histone octamer back-and-forth by a total distance of more than 200 bp and switch directions more than 20 times on average before dissociation.

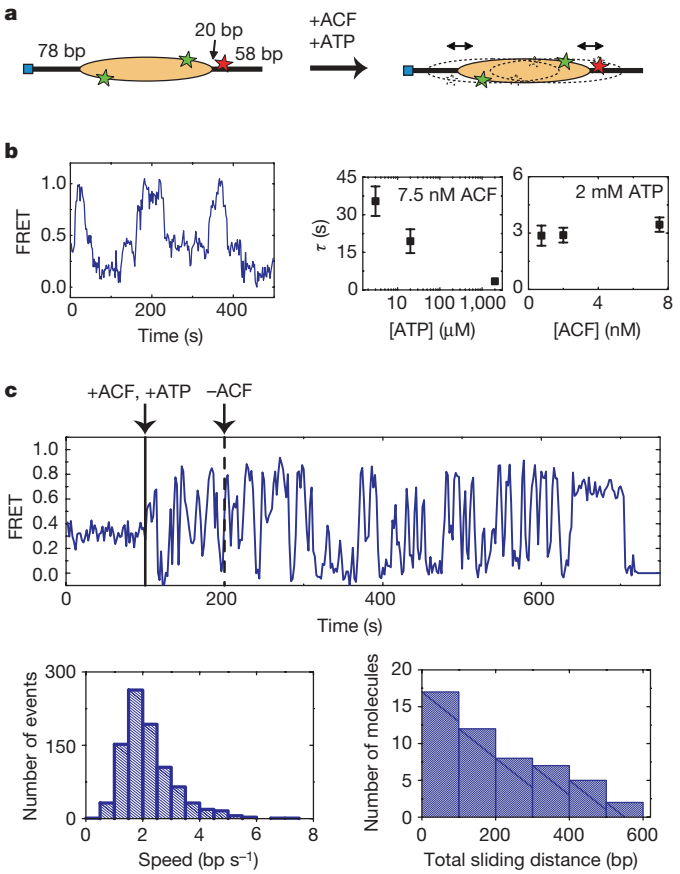

Figure 4 | ACF catalyses processive and bidirectional nucleosome translocation. a, A centre-positioned nucleosome flanked by 78 bp of linker DNA on both sides is subject to remodelling. **b**, FRET trace of a nucleosome in equilibrium with 7.5 nM ACF and 3 μM ATP showing back-and-forth translocation on DNA(left panel); the characteristic time of the FRET fluctuations (τ) depends on ATP, but not on ACF, concentration (right panel). The τ values were derived from autocorrelation analysis as described in Methods. **c**, Upper panel, a FRET trace showing processive and bidirectional nucleosome translocation by a continuously bound ACF complex. ACF (3 nM) and ATP (2 mM) were added at the time indicated by the solid black line. Unbound ACF (but not ATP) was then removed from the solution at the time indicated by the dashed black line. Lower left panel distribution of the translocation speed within each segment of unidirectional translocation. Lower right panel, distribution of the cumulative distance travelled by individual nucleosomes after removal of unbound ACF. Estimate of the travelling speed and distance is described in Methods. Error bars are ± s.e.m.

Statistical analyses indicate that the bidirectional remodelling is most probably caused by ACF dimers. The processive and bidirectional translocation of nucleosomes potentially allows ACF to rapidly sample the DNA on both sides of the nucleosome to generate regular inter-nucleosomal spacing.

METHODS SUMMARY

Briefly, various mononucleosome constructs, with different DNA sequences, DNA linker lengths and ssDNA gap locations, were reconstituted using histone octamers that were labelled with a green FRET donor dye (Cy3) and double stranded DNA that was labelled with a red FRET acceptor dye (Cy5) and a biotin. The nucleosomes were then anchored to a microscope slide via a biotin–streptavidin linkage. Unlabelled ACF or ACF labelled with a blue dye (Alexa 488) were added to the surface-anchored nucleosomes together with ATP to induce remodelling. The fluorescence signals from Alexa 488, Cy3 and Cy5 were detected by a TIRF microscope, separated by dichroic mirrors, and imaged onto separate areas of an amplified-CCD camera after passing through various fluorescence emission filters. Custom-written software was used to identify single nucleosomes on the slide and to monitor the Alexa 488, Cy3 and Cy5 fluorescence at these positions for extended periods of time. The FRET value was defined as $I_A/(I_D + I_A)$, where I_D and I_A represent the fluorescence signals detected in the Cy3 and Cy5 channels, respectively.

Full Methods and any associated references are available in the online version of the paper at www.nature.com/nature.

Received 13 August; accepted 2 November 2009.

1. Becker, P. B. & Horz, W. ATP-dependent nucleosome remodeling. *Annu. Rev. Biochem.* **71,** 247–273 (2002).
2. Narlikar, G. J., Fan, H. Y. & Kingston, R. E. Cooperation between complexes that regulate chromatin structure and transcription. *Cell* **108,** 475–487 (2002).
3. Flaus, A. & Owen-Hughes, T. Mechanisms for ATP-dependent chromatin remodelling: farewell to the tuna-can octamer? *Curr. Opin. Genet. Dev.* **14,** 165–173 (2004).
4. Smith, C. L. & Peterson, C. L. ATP-dependent chromatin remodeling. *Curr. Top. Dev. Biol.* **65,** 115–148 (2004).
5. Clapier, C. R. & Cairns, B. R. The biology of chromatin remodeling complexes. *Annu. Rev. Biochem.* **78,** 273–304 (2009).
6. Saha, A., Wittmeyer, J. & Cairns, B. R. Chromatin remodeling by RSC involves ATP-dependent DNA translocation. *Genes Dev.* **16,** 2120–2134 (2002).
7. Whitehouse, I., Stockdale, C., Flaus, A., Szczelkun, M. D. & Owen-Hughes, T. Evidence for DNA translocation by the ISWI chromatin-remodeling enzyme. *Mol. Cell. Biol.* **23,** 1935–1945 (2003).
8. Tsukiyama, T., Palmer, J., Landel, C. C., Shiloach, J. & Wu, C. Characterization of the Imitation Switch subfamily of ATP-dependent chromatin-remodeling factors in *Saccharomyces cerevisiae*. *Genes Dev.* **13,** 686–697 (1999).
9. Hamiche, A., Sandaltzopoulos, R., Gdula, D. A. & Wu, C. ATP-dependent histone octamer sliding mediated by the chromatin remodeling complex NURF. *Cell* **97,** 833–842 (1999).
10. Längst, G., Bonte, E. J., Corona, D. F. & Becker, P. B. Nucleosome movement by CHRAC and ISWI without disruption or trans-displacement of the histone octamer. *Cell* **97,** 843–852 (1999).
11. Kassabov, S. R., Henry, N. M., Zofall, M., Tsukiyama, T. & Bartholomew, B. High-resolution mapping of changes in histone-DNA contacts of nucleosomes remodeled by ISW2. *Mol. Cell. Biol.* **22,** 7524–7534 (2002).
12. Zhang, Y. *et al.* DNA translocation and loop formation mechanism of chromatin remodeling by SWI/SNF and RSC. *Mol. Cell* **24,** 559–568 (2006).
13. Lia, G. *et al.* Direct observation of DNA distortion by the RSC complex. *Mol. Cell* **21,** 417–425 (2006).
14. Shundrovsky, A., Smith, C. L., Lis, J. T., Peterson, C. L. & Wang, M. D. Probing SWI/SNF remodeling of the nucleosome by unzipping single DNA molecules. *Nature Struct. Mol. Biol.* **13,** 549–554 (2006).
15. Stryer, L. & Haugland, R. P. Energy transfer: a spectroscopic ruler. *Proc. Natl Acad. Sci. USA* **58,** 719–726 (1967).
16. Ha, T. *et al.* Probing the interaction between two single molecules: fluorescence resonance energy transfer between a single donor and a single acceptor. *Proc. Natl Acad. Sci. USA* **93,** 6264–6268 (1996).
17. Zhuang, X. *et al.* A single molecule study of RNA catalysis and folding. *Science* **288,** 2048–2051 (2000).
18. Ito, T., Bulger, M., Pazin, M. J., Kobayashi, R. & Kadonaga, J. T. ACF, an ISWI-containing and ATP-utilizing chromatin assembly and remodeling factor. *Cell* **90,** 145–155 (1997).
19. Ito, T. *et al.* ACF consists of two subunits, Acf1 and ISWI, that function cooperatively in the ATP-dependent catalysis of chromatin assembly. *Genes Dev.* **13,** 1529–1539 (1999).
20. Bochar, D. A. *et al.* A family of chromatin remodeling factors related to Williams syndrome transcription factor. *Proc. Natl Acad. Sci. USA* **97,** 1038–1043 (2000).
21. LeRoy, G., Loyola, A., Lane, W. S. & Reinberg, D. Purification and characterization of a human factor that assembles chromatin. *J. Biol. Chem.* **275,** 14787–14790 (2000).
22. Poot, R. A. *et al.* HuCHRAC, a human ISWI chromatin remodelling complex contains hACF1 and two novel histone-fold proteins. *EMBO J.* **19,** 3377–3387 (2000).
23. Yang, J. G., Madrid, T. S., Sevastopoulos, E. & Narlikar, G. J. The chromatin-remodeling enzyme ACF is an ATP-dependent DNA length sensor that regulates nucleosome spacing. *Nature Struct. Mol. Biol.* **13,** 1078–1083 (2006).
24. Lowary, P. T. & Widom, J. New DNA sequence rules for high affinity binding to histone octamer and sequence-directed nucleosome positioning. *J. Mol. Biol.* **276,** 19–42 (1998).
25. Abbondanzieri, E. A. *et al.* Dynamic binding orientations direct activity of HIV reverse transcriptase. *Nature* **453,** 184–189 (2008).
26. He, X., Fan, H. Y., Narlikar, G. J. & Kingston, R. E. Human ACF1 alters the remodeling strategy of SNF2h. *J. Biol. Chem.* **281,** 28636–28647 (2006).
27. Stockdale, C., Flaus, A., Ferreira, H. & Owen-Hughes, T. Analysis of nucleosome repositioning by yeast ISWI and Chd1 chromatin remodeling complexes. *J. Biol. Chem.* **281,** 16279–16288 (2006).
28. Schwanbeck, R., Xiao, H. & Wu, C. Spatial contacts and nucleosome step movements induced by the NURF chromatin remodeling complex. *J. Biol. Chem.* **279,** 39933–39941 (2004).

29. Zofall, M., Persinger, J., Kassabov, S. R. & Bartholomew, B. Chromatin remodeling by ISW2 and SWI/SNF requires DNA translocation inside the nucleosome. *Nature Struct. Mol. Biol.* **13,** 339–346 (2006).
30. Dang, W. & Bartholomew, B. Domain architecture of the catalytic subunit in the ISW2-nucleosome complex. *Mol. Cell. Biol.* **27,** 8306–8317 (2007).
31. Li, G., Levitus, M., Bustamante, C. & Widom, J. Rapid spontaneous accessibility of nucleosomal DNA. *Nature Struct. Mol. Biol.* **12,** 46–53 (2004).
32. Partensky, P. D. & Narlikar, G. J. Chromatin remodelers act globally, sequence positions nucleosomes locally. *J. Mol. Biol.* **391,** 12–25 (2009).
33. Luger, K., Mader, A. W., Richmond, R. K., Sargent, D. F. & Richmond, T. J. Crystal structure of the nucleosome core particle at 2.8 Å resolution. *Nature* **389,** 251–260 (1997).
34. Fyodorov, D. V. & Kadonaga, J. T. Dynamics of ATP-dependent chromatin assembly by ACF. *Nature* **418,** 896–900 (2002).
35. Gangaraju, V. K., Prasad, P., Srour, A., Kagalwala, M. N. & Bartholomew, B. Conformational changes associated with template commitment in ATP-dependent chromatin remodeling by ISW2. *Mol. Cell* **35,** 58–69 (2009).
36. Raki, L. R. The chromatin remodeller ACF acts as a dimeric motor to space nucleosomes. *Nature* doi:10.1038/nature08621 (this issue).
37. Strohner, R. *et al.* A 'loop recapture' mechanism for ACF-dependent nucleosome remodeling. *Nature Struct. Mol. Biol.* **12,** 683–690 (2005).
38. Fitzgerald, D. J. *et al.* Reaction cycle of the yeast Isw2 chromatin remodeling complex. *EMBO J.* **23,** 3836–3843 (2004).
39. Cairns, B. R. Chromatin remodeling: insights and intrigue from single-molecule studies. *Nature Struct. Mol. Biol.* **14,** 989–996 (2007).

Supplementary Information is linked to the online version of the paper at www.nature.com/nature.

Acknowledgements We thank J. Widom for providing the plasmid containing the 601 positioning sequence and R. E. Kingston for the plasmids containing the *SNF2h* and *Acf1* genes. We also thank L. Racki and E. Abbondanzieri for helpful discussions, and W. Huang and B. Harada for help with some experiments. This work is supported in part by Howard Hughes Medical Institute (to X.Z.) and the National Institutes of Health (GM073767) and the Beckman Foundation (to G.J.N). X.Z. is a Howard Hughes Medical Institute investigator. M.D.S. was a NIH Ruth L. Kirschstein NSRA Fellow, G.J.N is a Leukemia and Lymphoma Society Scholar.

Author Contributions T.R.B. performed the experiments and analysis with help from M.D.S.; J.G.Y. made the enzymes and histone proteins. T.R.B., G.J.N. and X.Z. designed the experiments. X.Z. oversaw the project.

Author Information Reprints and permissions information is available at www.nature.com/reprints. Correspondence and requests for materials should be addressed to X.Z. (zhuang@chemistry.harvard.edu) and G.J.N (geeta.narlikar@ucsf.edu).

METHODS

Preparation of mononucleosomes. Various double-stranded (ds) DNA constructs with different sequences and flanking linker lengths, as shown in Supplementary Fig. 1, were made by PCR and purified by PAGE. When needed, two-nucleotide (nt) single-stranded DNA (ssDNA) gaps were generated in the dsDNA by excision of two adjacent deoxyuridine residues by the Uracil-Specific Excision Reagent (USER, New England Biolabs), which contains a mixture of uracil DNA glycosylase and endonuclease VIII[29]. Before USER digestion, the full-length dsDNA was constructed by ligation of two separate, PAGE-purified, PCR products with complementary sticky ends made by restriction digestion. Deoxyuridine, 5′-Cy5 and 5′-biotin modifications were incorporated synthetically into PCR primers (Integrated DNA Technologies). For internal Cy5 labelling, PCR primers containing an internal amino modifier (dT C6) (Integrated DNA Technologies) were labelled with a monoreactive Cy5 (GE Healthcare) and purified by reverse-phase HPLC over a C8 column (GE Healthcare) before use in PCR.

To label the histone H2A protein with the FRET donor, a unique cysteine substitution was introduced to residue 120 of H2A. A Cy3 dye (GE Healthcare) was attached to the cysteine as described previously[23]. The Cy3-labelled and unlabelled H2A were mixed at a ratio of 1:1 together with other histone proteins (H2B, H3 and H4) to form histone octamers. Mononucleosomes were reconstituted from DNA and octamers by salt gradient dialysis and purified by ultracentrifugation over a 10–30% (v/v) glycerol gradient[40]. Without addition of the remodelling enzyme, the FRET values from the nucleosomes remained unchanged for at least one hour after the nucleosomes were anchored to the surface, indicating that the nucleosomes were stable during this time scale.

Preparation of ACF. The procedure to prepare ACF was previously described[23,41]. Briefly, haemagglutinin (HA)–Acf1 and Flag–SNF2h were individually overexpressed in Sf9 cells using a baculovirus expression system. Excess HA-tagged Acf1 extract was mixed with Flag-tagged SNF2h extract, and the ACF complex was purified using M2-affinity chromatography[41]. For experiments that directly monitor the binding of ACF to nucleosomes, we labelled the ACF complex with the Alexa 488 dye. Before M2 elution, the resin was washed with labelling buffer (20% glycerol, 20 mM HEPES pH 7.0, 0.2 mM EDTA, 100 mM KCl, 1 mM benzamidine HCl, 1 mM TCEP) followed by addition of Alexa 488 maleimide (Molecular Probes) to 100 μM final concentration. After 30 min at 4 °C, the labelling reaction was quenched with 80 mM β-mercaptoethanol for 15 min. The resin was washed extensively with wash buffer (20% glycerol, 20 mM HEPES pH 7.9, 0.2 mM EDTA, 100 mM KCl, 1 mM benzamidine HCl, 1 mM DTT) and the protein was then eluted. Stoichiometry of Acf1 to SNF2h was confirmed by SYPRO staining.

Single-nucleosome FRET measurements. Quartz microscope slides were coated with methoxy-poly(ethylene glycol) (PEG, Nektar Therapeutics or Laysan Bio), biotin-PEG (Nektar Therapeutics or Laysan Bio) and streptavidin as described previously[25]. The biotinylated nucleosomes were then linked to the streptavidin-coated slide surface via a biotin-streptavidin linkage. The donor and acceptor fluorescence signals from the surface-anchored nucleosomes were excited with a 532 nm Nd:YAG (neodymium-doped yttrium aluminium garnet) laser (CrystaLaser) in the total internal refection geometry and fluorescence emission from Cy3 and Cy5 was detected with a ×60 water immersion objective (Olympus), filtered with a 550 nm long-pass filter (Chroma Technology), spectrally spilt by a 630 nm dichroic mirror (Chroma Technology), and imaged onto two halves of a CCD camera (Andor iXon 897 or iXon^{EM}+ 888; ref. 25). Unlabelled ACF was added to the surface-anchored nucleosomes together with ATP to induce remodelling. In experiments that monitored both the binding of ACF and the remodelling of nucleosomes, ACF labelled with Alexa 488 was added to the nucleosomes. Alexa 488 and Cy3 were excited by alternating 488 nm argon ion and 532 nm Nd:YAG laser lines, respectively.

Because the FRET donor Cy3 is attached to the H2A subunit of the histone octamer, the presence of two H2A subunits in each octamer led to a heterogeneous population of nucleosomes with three different labelling configurations: (1) donor on the H2A subunit proximal to the acceptor, yielding a high FRET level, (2) donor on the distal H2A, yielding a lower FRET level, (3) donor on both H2A subunits, yielding an intermediate FRET value. For example, three distinct peaks centred at FRET = 0.88, 0.75 and 0.58 were observed in the FRET distribution of the nucleosomes with exit linker length $n = 3$ bp (Fig. 1b). In this work, we focus our analyses on nucleosomes containing a single donor on the proximal H2A. In the FRET histogram analysis, the histograms were fit with three Gaussian peaks and the peak with the highest FRET value was selected. In the FRET trace analysis, traces starting with a mean FRET > 0.75 and exhibiting a single donor bleaching step were selected. This selection process allowed us to include the entire population of nucleosomes with a donor on the proximal H2A without contamination from nucleosomes with donor on both H2A subunits, which exhibit two donor bleaching steps. Such selection process indeed resulted in a single population of nucleosomes with FRET centred at 0.88 (Supplementary Fig. 2e). Similar selection criteria were used for nucleosomes with exit linker length $n = 6$ bp, 0 bp and -3 bp: Traces starting with a mean FRET larger than a threshold value (0.6 for $n = 6$ bp, 0.75 for $n = 0$ bp and $n = -3$ bp) and exhibiting a single donor bleaching step were selected for further analysis. To generate the calibration curve in Fig. 1c, nucleosomes with $n = 3, 6, 8, 10, 11, 13, 18$ and 23 bp were used. The FRET distributions in each case were fit to three Gaussians and the peak with the highest FRET value was selected, except for the $n = 18$ or 23 bp nucleosomes, which exhibited only very low FRET values that appeared as one peak. In these two latter cases, the FRET distribution was fit to a single Gaussian function to extract the peak position.

In experiments where buffer exchange was used to add or remove ACF and ATP, the sample chamber was infused with new buffer using a syringe pump (KD Scientific). To ensure complete buffer exchange within the sample chamber (~20 μl), a large excess of the new buffer was flown through the chamber on infusion. In the case of ACF and ATP addition, 300 μl or ~15 chamber volumes of new buffer was infused. In the case of ACF removal, 600 μl of new buffer was infused. The dead time for buffer exchange was measured to be 1.3 s.

Nucleosomes were imaged at 30 °C in a buffer consisting of 12 mM HEPES, 40 mM Tris pH 7.5, 60 mM KCl, 0.32 mM EDTA, 3 mM $MgCl_2$, 10% glycerol, 0.02% Igepal (Sigma Aldrich), an oxygen scavenging system (10% glucose, 800 μg ml^{-1} glucose oxidase, 40 μg ml^{-1} catalase) to reduce photobleaching, 2 mM Trolox (Sigma) to reduce photoblinking of the dyes[42], and 0.1 mg ml^{-1} BSA (Promega) to prevent non-specific sticking of nucleosomes and ACF to the surface.

Estimate of the characteristic oscillation time, the translocation speed and the total travelling distance of centre-positioned nucleosomes. The characteristic FRET fluctuation time (τ) of the centre-positioned nucleosomes in the presence of ACF and ATP was derived using autocorrelation analysis. Briefly, the autocorrelation function at each condition was constructed from ~100 FRET time traces. The characteristic time τ was derived as the decay constant from single exponential fitting of the autocorrelation function.

To estimate the cumulative distance (not net distance) of nucleosome translocation on DNA induced by a bound ACF complex as shown in Fig. 4c, FRET traces during the period after removal of ACF from the solution but before dissociation of the bound ACF from the nucleosome were divided into unidirectional segments of monotonically changing FRET. The FRET change in each segment was converted into the number of base pairs translocated by comparison with the calibration curve shown in Fig. 1c. The results from all segments of a trace were summed to give the total distance travelled by the octamer. The following reasons make the estimated total distance an approximate, lower bound estimate of the cumulative distance travelled by the histone octamer: (1) only unidirectional segments with a FRET change greater than 0.3 were selected for the sum to avoid counting noise in the FRET signal. To characterize noise, FRET fluctuations from the nucleosomes in the absence of ACF were analysed and the probability of observing a FRET change greater than 0.3 in the absence of ACF was found to be less than 0.002. Therefore, 0.3 is a rather conservative threshold for nucleosome translocation, leading to an underestimate of travelling distance. (2) The slope of the calibration curve in Fig. 1c was used to estimate distances from changes in FRET, but as the FRET value gets near 0 or 1, it saturates and becomes an insensitive measure of distance, also causing an underestimate. The possibility that the DNA trajectories within the nucleosome or on the entry side could differ from that of the exit linker DNA may give additional error in the distance estimate. To estimate the speed of octamer translocation, the distance change within each unidirectional segment determined above was divided by the duration of the segment. To determine the number of times a nucleosome switched its direction, only events switching from a decreasing trend to an increasing trend in FRET were counted, as the switching from an increasing trend to a decreasing trend could be due to the FRET acceptor on the DNA passing by the FRET donor on the octamer without switching direction. Therefore, the estimated number of switching times is also an underestimate, as some of the latter type of switching events may also represent real directional switching of the nucleosome translocation.

40. Luger, K., Rechsteiner, T. J. & Richmond, T. J. Preparation of nucleosome core particle from recombinant histones. *Methods Enzymol.* **304**, 3–19 (1999).
41. Aalfs, J. D., Narlikar, G. J. & Kingston, R. E. Functional differences between the human ATP-dependent nucleosome remodeling proteins BRG1 and SNF2H. *J. Biol. Chem.* **276**, 34270–34278 (2001).
42. Rasnik, I., McKinney, S. A. & Ha, T. Nonblinking and long-lasting single-molecule fluorescence imaging. *Nature Methods* **3**, 891–893 (2006).